Two different mechanisms of stabilization of regular π-stacks of radicals in switchable dithiazolyl-based materials

Tommaso Francese[a,b,‡], Sergi Vela[c], Mercè Deumal[a], Fernando Mota[a], Juan J. Novoa[a], Matteo Farnesi Camellone[d], Stefano Fabris[d], Remco W.A. Havenith[b,e], Ria Broer[b], Jordi Ribas-Arino[a,*]

[a] *Departament de Ciència dels Materials i Química Física and IQTCUB, Universitat de Barcelona, Martí i Franquès 1, Barcelona, E-08028, Spain*.

[b] *Theoretical Chemistry, Zernike Institute for Advance Materials, University of Groningen, Nijenborgh 4, 9747 AG Groningen, The Netherlands*

[c] *Laboratory for Computational Molecular Design, Institute of Chemical Sciences and Engineering, EPFL, CH- 1015 Lausanne, Switzerland*

[d] *CNR-IOM, Consiglio Nazionale delle Ricerche–Istituto Officina dei Materiali, c/o SISSA, via Bonomea 265, 34136 Trieste, Italy*

[e] *Stratingh Institute for Chemistry, University of Groningen, 9747 AG Groningen, The Netherlands*

‡ *Present address: Pritzker School of Molecular Engineering, The University of Chicago, Eckhardt Research Center 5640 S. Ellis Ave. ACC 205, Chicago, IL, USA*

-ELECTRONIC SUPPLEMENTARY INFORMATION-

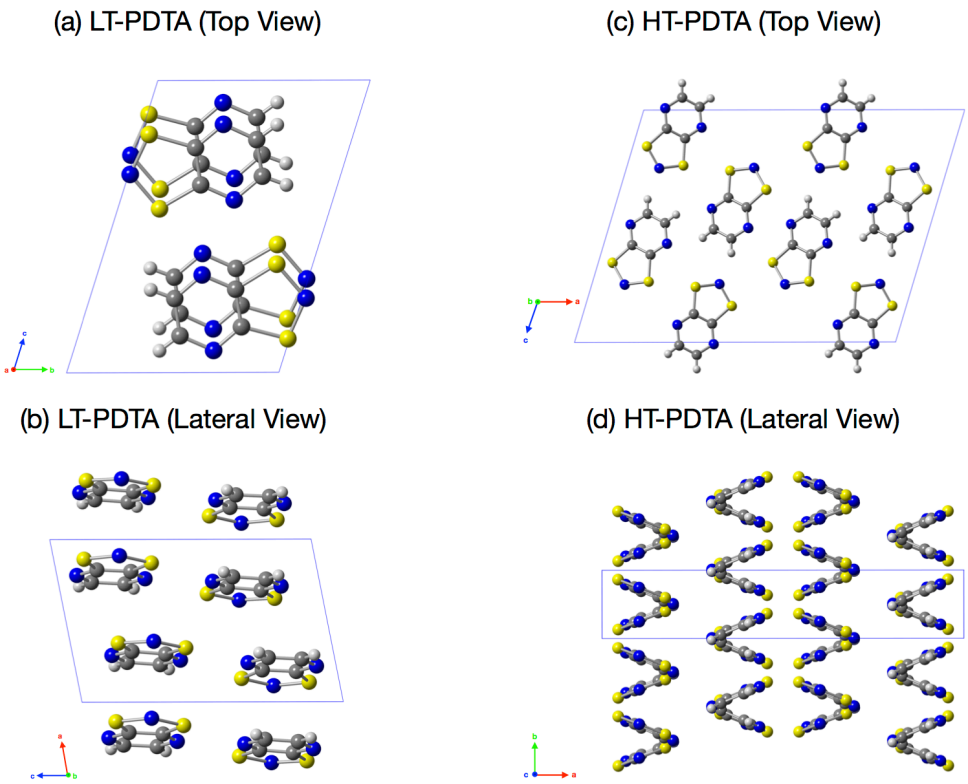

Figure S1. Different views of the crystal packing of the LT (a-b) and HT (c-d) polymorphs of PDTA at 323 K. The CCDC refcodes of the LT and HT polymorphs are BEZQAZ03 and BEZQAZ02, respectively.

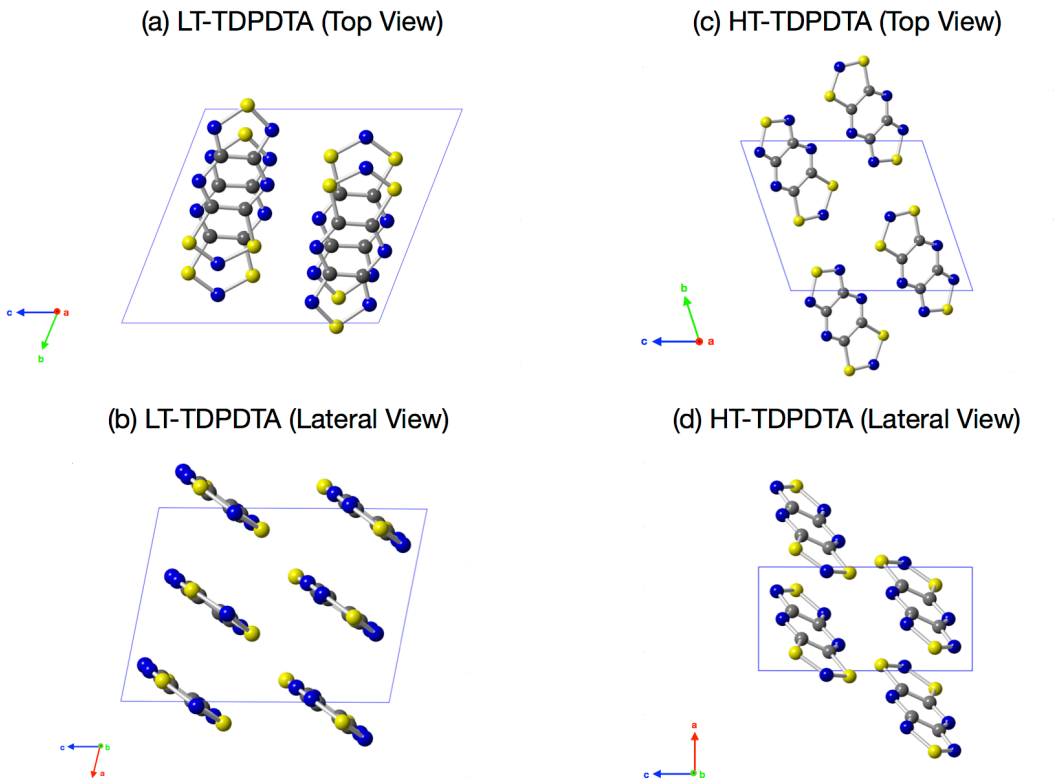

Figure S2. Different views of the crystal packing of the LT (a-b) and HT (c-d) polymorphs of TDPDTA at 150 and 293 K, respectively. The CCDC refcodes of the LT and HT polymorphs are NEWYET and NEWYET01, respectively.

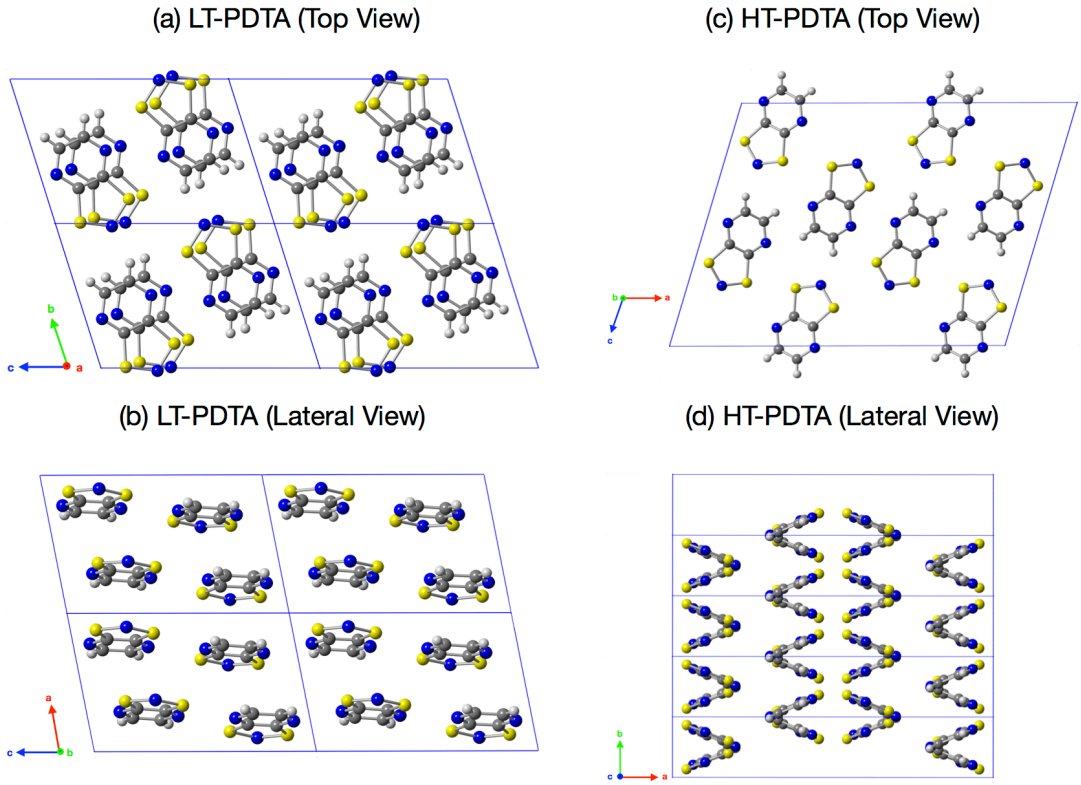

Figure S3. Different views of the supercells used in the optimizations and simulations of the LT (a-b) and HT (c-d) polymorphs of PDTA. The supercell for LT was constructed by duplicating the unit cell in all three spatial directions. The supercell for HT, in turn, was constructed by replicating the unit cell in two of the spatial directions. Specifically, the relations between the supercell (sc) vectors and the unit cell (uc) vectors are: $a_{sc} = 2 \cdot a_{uc}$; $b_{sc} = 4 \cdot b_{uc}$; $c_{sc} = c_{uc}$.

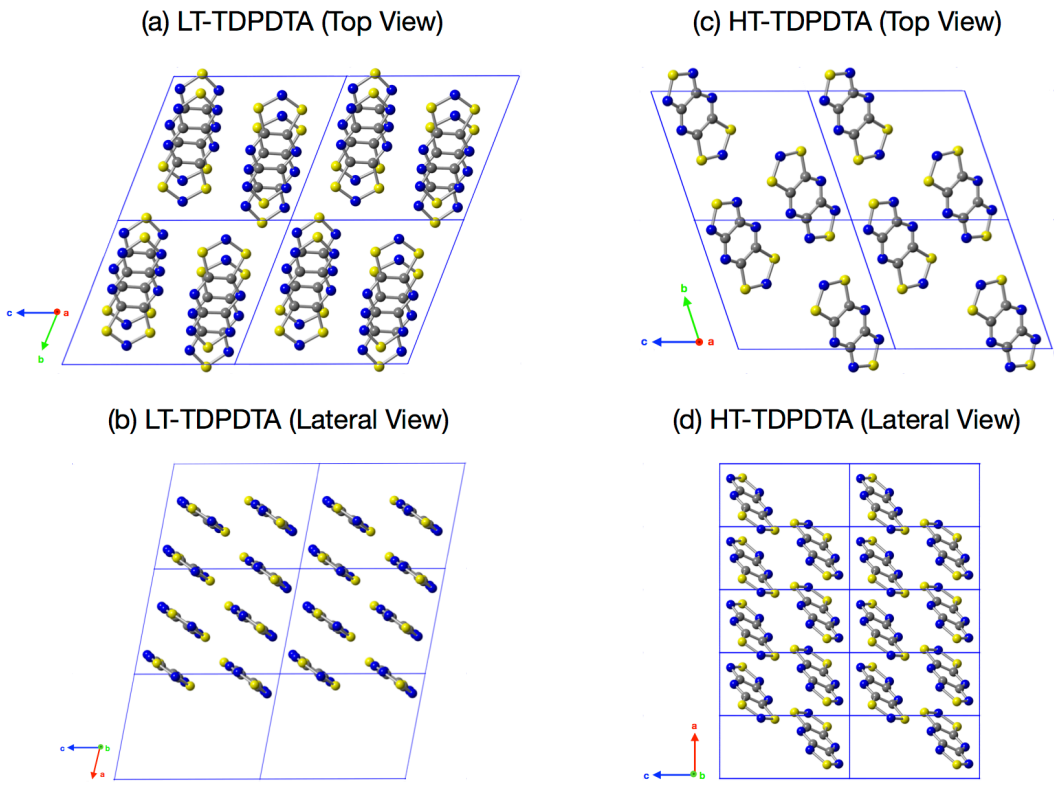

Figure S4. Different views of the supercells used in the optimizations and simulations of the LT (a-b) and HT (c-d) polymorphs of TDPDTA. The supercell for LT was constructed by duplicating the unit cell in all three spatial directions. The supercell for HT, in turn, was constructed by replicating the unit cell in the three spatial directions. Specifically, the relations between the supercell (sc) vectors and the unit cell (uc) vectors are: $a_{sc} = 4 \cdot a_{uc}$; $b_{sc} = 2 \cdot b_{uc}$; $c_{sc} = 2 \cdot c_{uc}$.

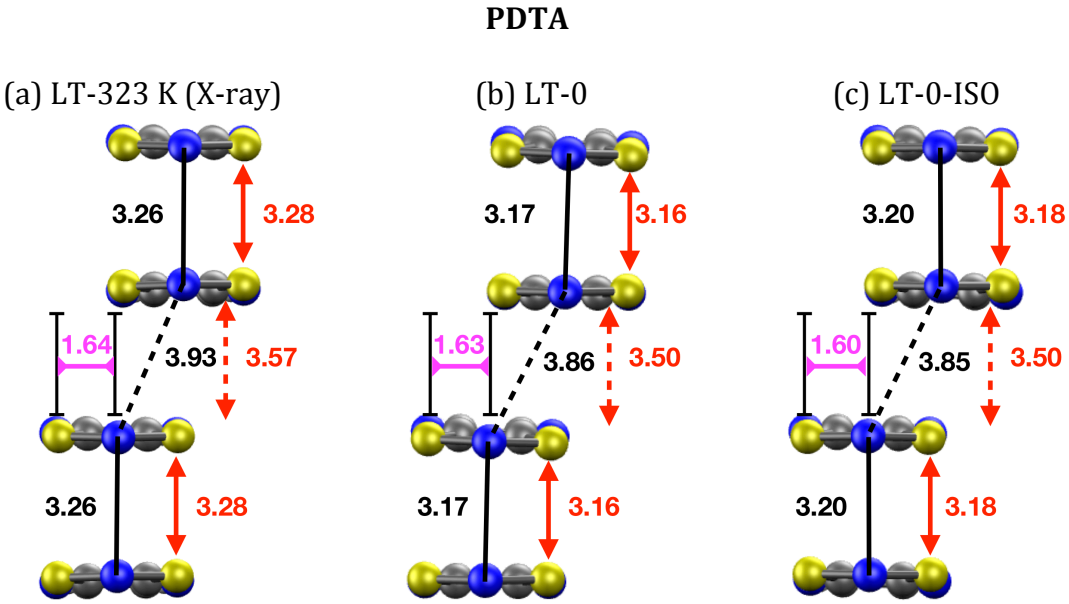

Figure S5. Side view of one π-stack of the LT polymorph of PDTA. The figure displays (*a*) the X-ray structure at 323 K, (*b*) the optimized structure at 0 K and (c) the optimized structure at 0 K of one isolated stack. The black, red and purple values shown in the image mark the distances between the nitrogen atoms of the S-N-S moieties of adjacent radicals, the interplanar distance (d_{IP}) between adjacent radicals and the degree of latitudinal slippage between adjacent radicals (d_{SL}), respectively.

TDPDTA

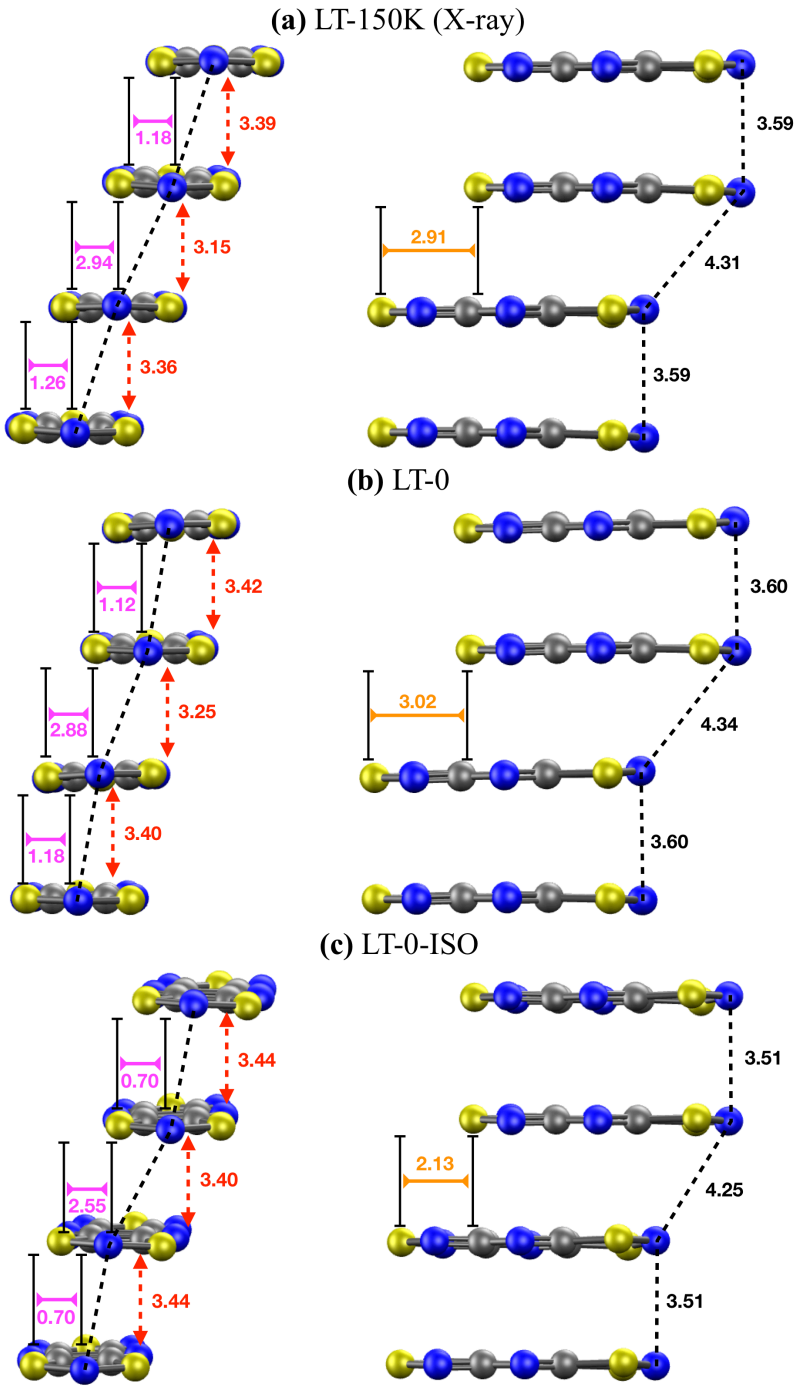

Figure S6. Two side views of one π-stack of the LT polymorph of TDPDTA. The figure displays (*a*) the X-ray structure at 293 K, (*b*) the optmized structure at 0 K and (*c*) the optimized structure at 0 K of one isolated stack. The black, red, purple and orange values shown in the image mark the distances between the nitrogen atoms of the S-N-S moieties of adjacent radicals, the interplanar distance between adjacent radicals (d_{IP}), the degree of latitudinal slippage between adjacent radicals (d_{SL}), and the degree of longitudinal slippage (d_{LG}), respectively.

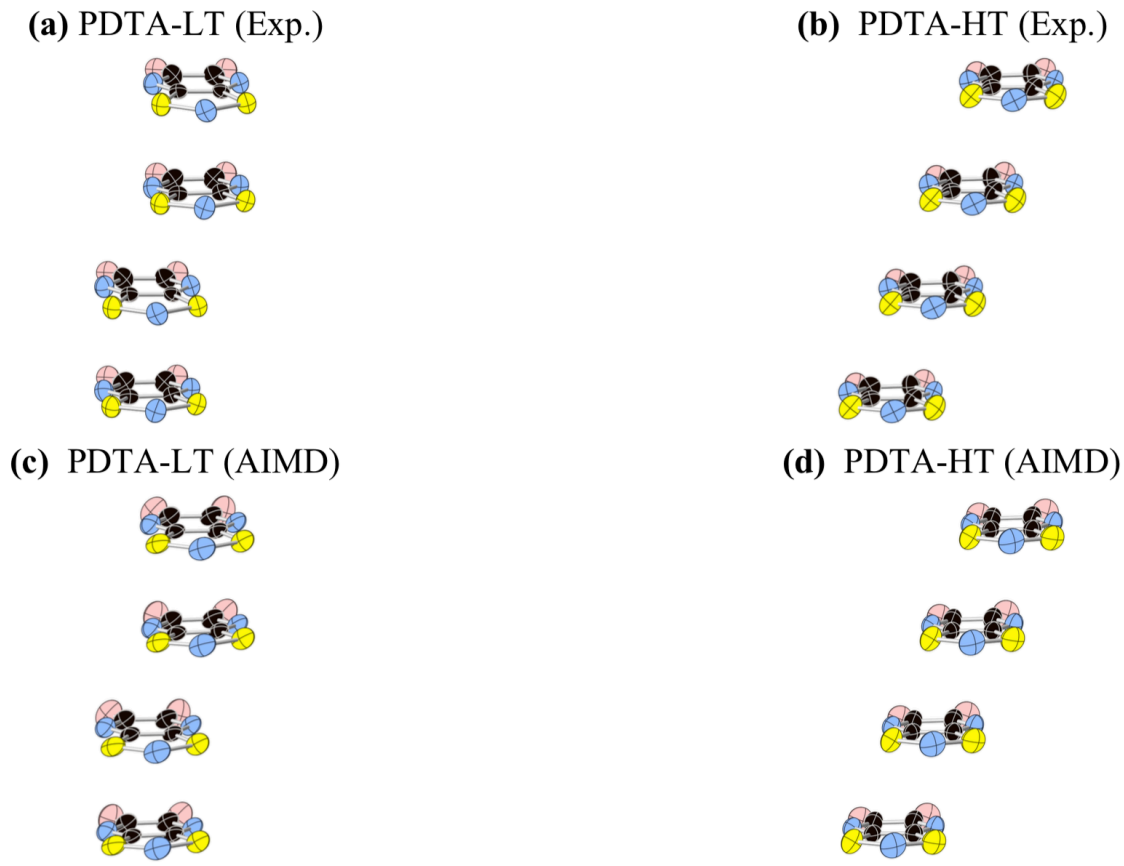

Figure S7. Thermal ellipsoids of the atoms of the PDTA radicals in the LT and HT polymorphs. *Top panels*: experimental thermal ellipsoids obtained from X-ray measurements. *Bottom panels*: thermal ellipsoids obtained from *ab initio* molecular dynamics (AIMD) simulations. The displayed ellipsoids correspond to a probability of 50%. Note that the computed thermal ellipsoids were obtained from AIMD simulations run at 300 K (HT) and 323 K (LT), respectively, while the experimental thermal ellipsoids were obtained from X-ray structures recorded at 323 K. The computed thermal ellipsoids were plotted on the basis of the data collected in Table S1.

(a) TDPDTA-LT (Exp.)

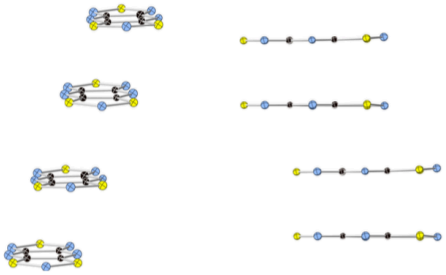

(b) TDPDTA-HT (Exp.)

(c) TDPDTA-LT (AIMD)

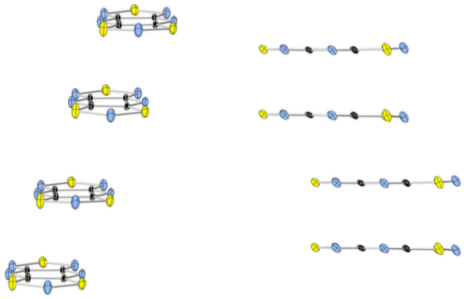

(d) TDPDTA-HT (AIMD)

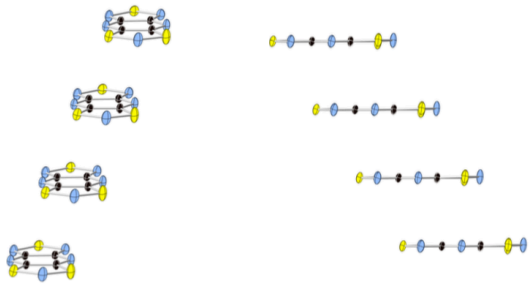

Figure S8. Thermal ellipsoids of the atoms of the TDPDTA radicals in the LT and HT polymorphs. *Top panels*: experimental thermal ellipsoids obtained from X-ray measurements made at 150 K (LT) and 293 K (HT). *Bottom panels*: thermal ellipsoids obtained from *ab initio* molecular dynamics (AIMD) simulations carried out at 150 K (LT) and 293 K (HT). The displayed ellipsoids correspond to a probability of 50%. The computed thermal ellipsoids were plotted on the basis of the data collected in Table S1.

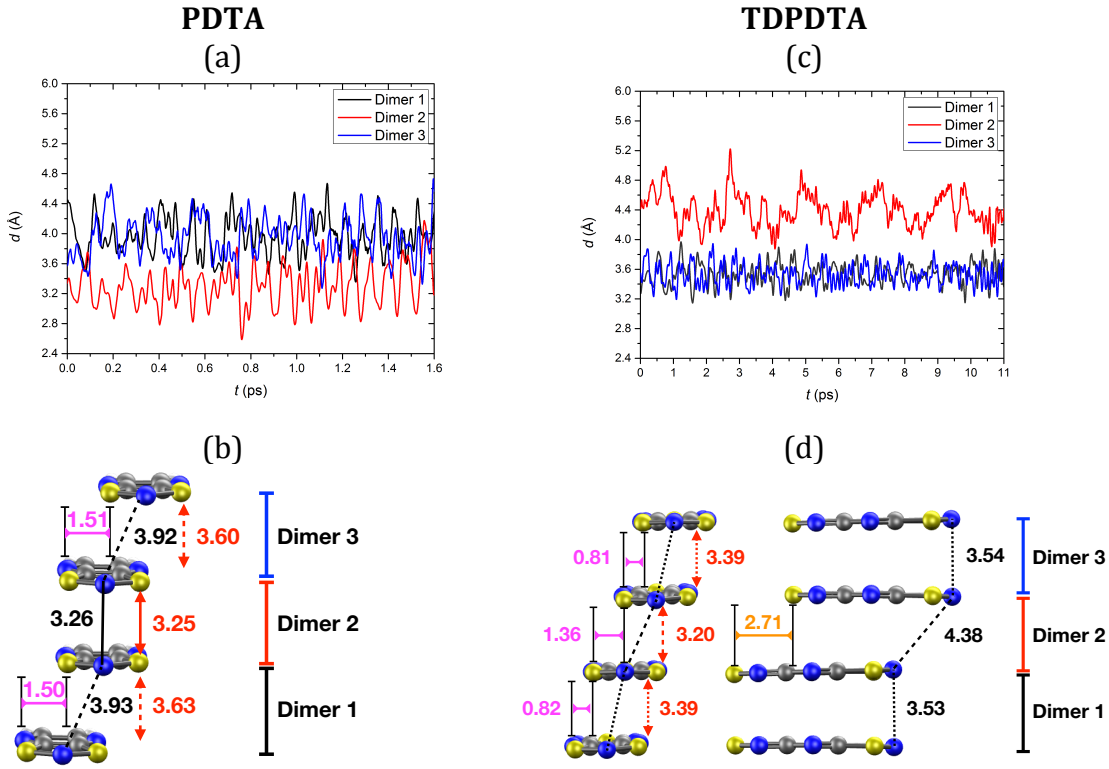

Figure S9. Results of the AIMD simulations of the LT polymorphs of PDTA (graphics on the left) and TDPDTA (graphics on the right). The simulations of PDTA and TDPDTA were run at 323 and 150 K, respectively. The panel shows: the time-resolved evolution of the distance between the nitrogen atoms of the S-N-S moieties of adjacent radicals in one column of (*a*) PDTA and one column of (*c*) TDPDTA; the average structure of one stack for both PDTA (*b*) and TDPDTA (*d*) as obtained from the AIMD simulations. Note that two different side views of one stack are displayed in the case of TDPDTA. The supercells used in the AIMD simulations of the LT polymorphs were built directly from the corresponding X-ray measured unit cell parameters.

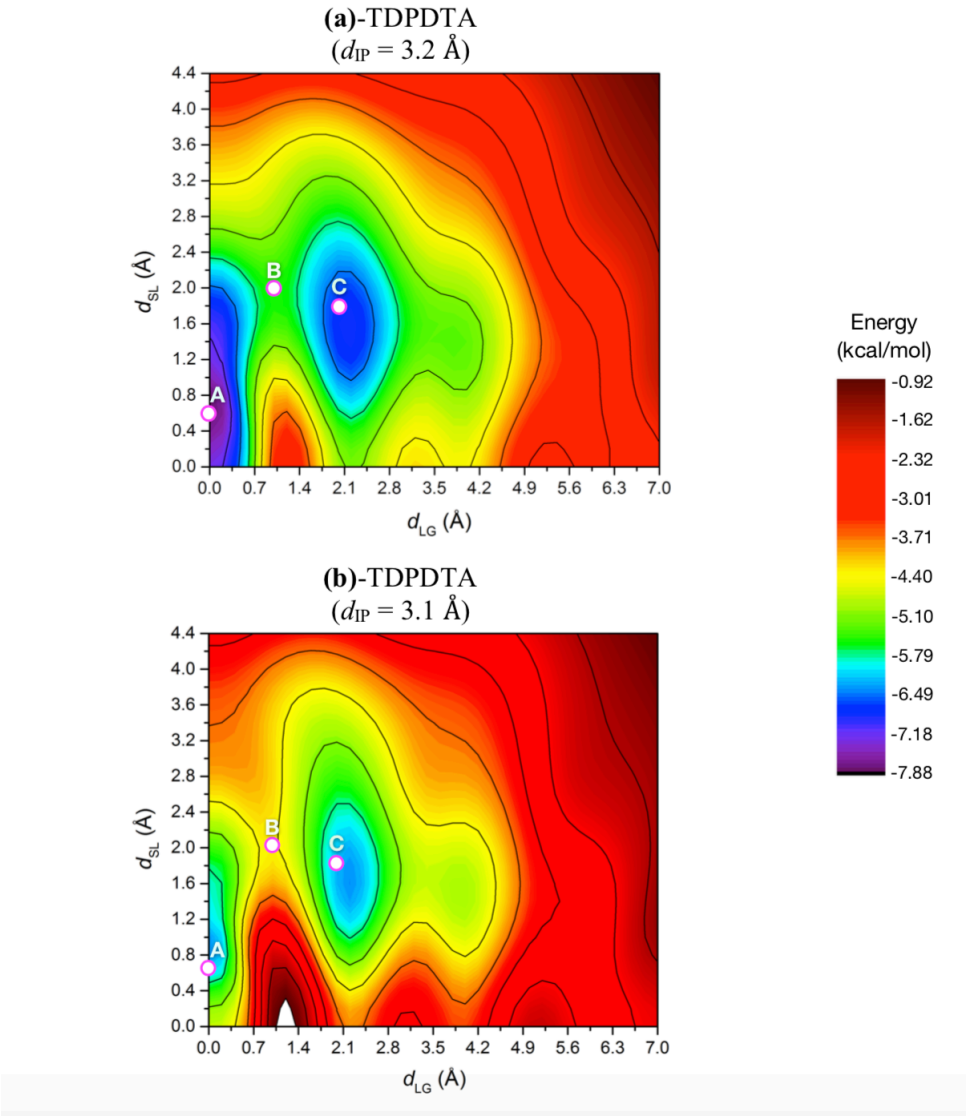

Figure S10. Potential energy surface of an isolated π-dimer of TDPDTA radicals as a function of the degree of latitudinal slippage (d_{SL}) and the degree of longitudinal slippage (d_{LG}), while keeping fixed the interplanar distance (d_{IP}) at two different values: (a) 3.2 Å and (b) 3.1 Å. The values of the energies refer to interaction energies between the two radicals. The configurations associated with the A and C points marked on the color map correspond to minimum energy configurations. The configuration marked with B corresponds to the transition state structure connecting the two minima.

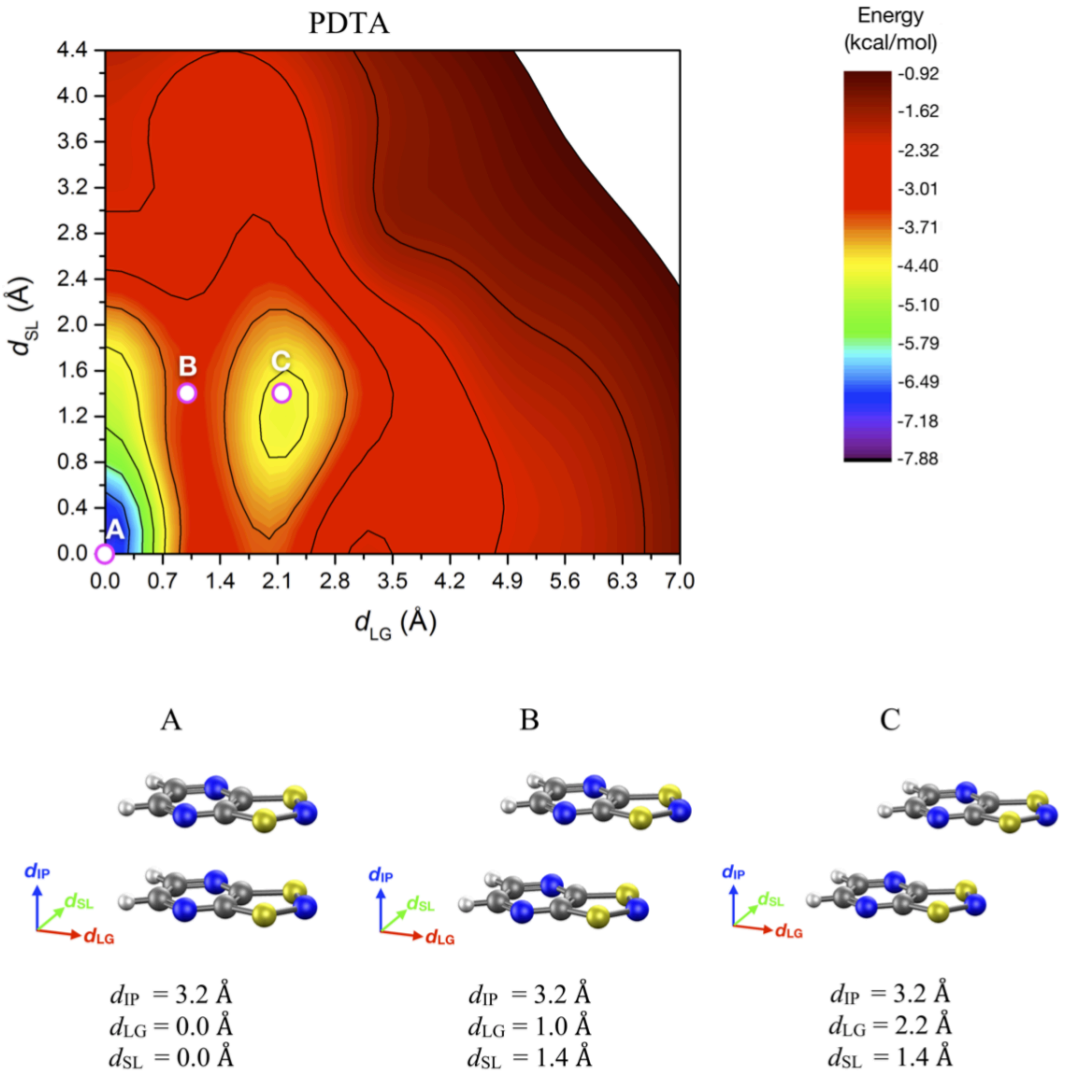

Figure S11. Potential energy surface of an isolated π-dimer of PDTA radicals as a function of the degree of latitudinal slippage (d_{SL}) and the degree of longitudinal slippage (d_{LG}), while keeping fixed the interplanar distance (d_{IP}) at a value of 3.2 Å. The values of the energies refer to interaction energies between the two radicals. The configurations associated with the A, B and C points marked on the color map are displayed at the bottom of the figure. The values of the d_{SL} and d_{LG} variables for each of these configurations are also shown.

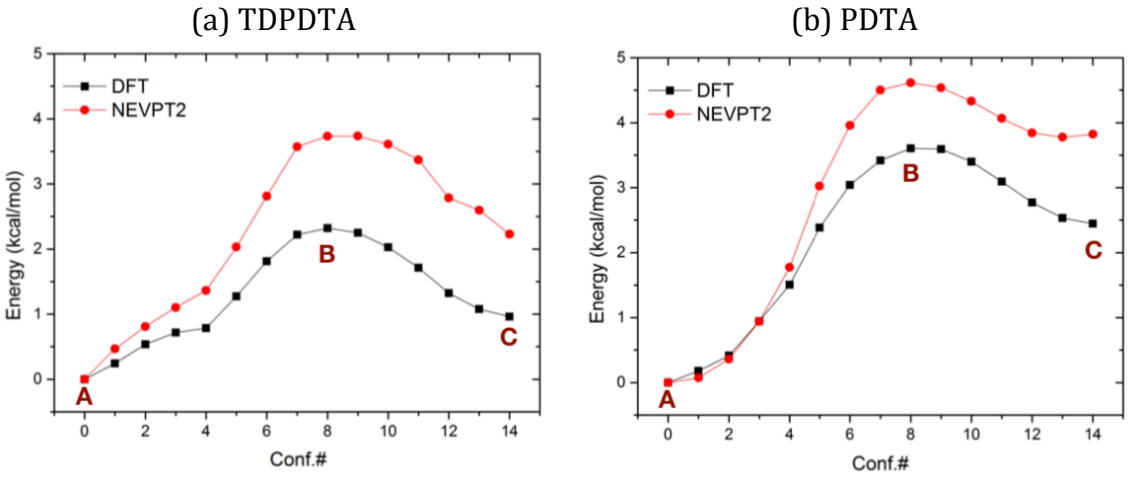

Figure S12. Minimum energy paths connecting configurations A and C through configuration B of (a) the 2D-PES of an isolated π-dimer of TDPDTA radicals displayed in Figure 9 and (b) the 2D-PES of an isolated π-dimer of PDTA radicals displayed in Figure S11. The energy profiles computed at the PBE-D2 level for both π-dimers have been benchmarked against profiles computed using a correlated wavefunction method (NEVPT2).

Table S1. Experimental and computed isotropic *B*-factors and anisotropic displacement parameters (U_{ij}) of the five atoms of the dithiazolyl ring for both polymorphs of PDTA and TDPDTA, and the HT polymorph of TTTA[a]. Only the diagonal element of the *U* tensor associated with the motion along the stacking direction is reported for each atom. All displacement parameters are given in Å^2.

			1-C		**2**-C		**3**-S		**4**-N		**5**-S	
TTTA[a]	HT$^{EXP.}$	(298K)[b,c]	U_{22}	B_{ISO}	U_{22}	B_{ISO}	U_{22}	B_{ISO}	U_{22}	B_{ISO}	U_{22}	B_{ISO}
			0.03	**2.31**	0.04	**2.37**	0.06	**3.25**	0.06	**3.32**	0.06	**3.08**
			U_{22}	B_{ISO}	U_{22}	B_{ISO}	U_{22}	B_{ISO}	U_{22}	B_{ISO}	U_{22}	B_{ISO}
PDTA	LT$^{EXP.}$	(323K) [b,c]	0.03	**2.50**	0.03	**2.65**	0.05	**3.61**	0.05	**3.68**	0.04	**3.25**
	LT^{AIMD}	(323K) [b]	0.03	**2.69**	0.04	**3.04**	0.05	**4.13**	0.06	**4.41**	0.05	**3.67**
	HT$^{EXP.}$	(323K) [b,c]	0.04	**2.83**	0.04	**3.16**	0.06	**4.49**	0.06	**4.42**	0.05	**4.14**
	HT^{AIMD}	(300K) [b]	0.04	**2.94**	0.04	**3.48**	0.07	**5.32**	0.07	**5.29**	0.06	**4.43**
			U_{11}	B_{ISO}	U_{11}	B_{ISO}	U_{11}	B_{ISO}	U_{11}	B_{ISO}	U_{11}	B_{ISO}
TDPDTA	LT$^{EXP.}$	(150K) [b,c]	0.01	**0.91**	0.01	**0.81**	0.01	**1.14**	0.02	**1.19**	0.01	**1.07**
	LT^{AIMD}	(150K) [b]	0.01	**0.85**	0.01	**0.85**	0.02	**1.30**	0.02	**1.33**	0.02	**1.30**
	HT$^{EXP.}$	(293K) [b,c]	0.02	**1.86**	0.02	**1.80**	0.03	**2.31**	0.03	**2.14**	0.03	**2.21**
	HT^{AIMD}	(293K) [b]	0.02	**1.21**	0.02	**1.21**	0.02	**1.67**	0.02	**1.66**	0.02	**1.66**

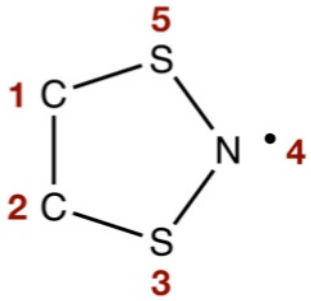

[a] In the case of TTTA, only the experimental displacement parameters are provided. The TTTA parameters have been included to allow for a comparison between the displacement parameters of a crystal exhibiting PED (TTTA or PDTA) and a crystal that does not exhibit PED (TDPDTA). Note that a direct comparison between PDTA and TDPDTA is not straightforward because the temperatures at which the X-ray structures of their HT phases were recorded differ by 30 K (the X-ray structures of the HT phases of PDTA and TDPDTA were recorded at 323 and 293 K, respectively). The temperatures at which the HT phases of TTTA and TDPDTA were recorded are much more similar (the HT phase of TTTA was recorded at 298 K). Therefore, a comparison between the thermal fluctuations of TTTA and TDPDTA is possible.

[b] Next to each polymorph, the temperature at which the X-ray structure was recorded or the temperature at which the AIMD simulation was performed is indicated.

[c] The experimental atomic displacement parameters of the different compounds were taken from the following references:
TTTA: *Nat. Commun*. **2014**, *5*, 4411.
PDTA: *J. Am. Chem. Soc*. **2004**, *126*, 14692-14693.
TDPDTA: *J. Am. Chem. Soc*. **1998**, *120*, 352 – 360.

Comment on the results collected in the Table S1: The larger experimental atomic displacement parameters (ADPs) and *B* factors of the HT phase PDTA compared to those of the HT phase of TDPDTA is consistent with the fact that the former compound exhibits PED while the latter compound does not. It might be argued that the larger ADPs and *B* factors of PDTA are just the result of the high temperature at which they were measured. However, a comparison between the experimental data of TTTA and TDPDTA clearly shows that the ADPs and *B* factors of the former are much larger than those of the latter even if the temperatures at which the parameters of both compounds were measured are very similar. It can thus be concluded that the presence of PED in a crystal yields larger ADPs and *B* factors.

Table S2. Energy decomposition analysis of the interaction energy between TDPDTA radicals in different configurations[a] of their isolated π-dimers. All components of the interaction energy are given in kcal mol^{-1}.

	Conf. A	Conf. B	Conf. C
Electrostatic	-10.84	-6.42	-5.27
Exchange	-9.62	-4.71	-3.83
Repulsion	56.73	27.50	23.77
Polarization	-17.22	-6.33	-5.93
DFT dispersion[b]	-17.24	-8.35	-8.39
Grimme dispersion[c]	-12.21	-8.83	-8.87
Total dispersion[d]	-29.45	-17.18	-17.26
Total interaction energy	-10,40	-7,15	-8,51

[a] The configurations are those marked by A, B and C in Figure 9 of the main text.
[b] This accounts for the dispersion that the PBE functional is able to recover by itself.
[c] This accounts for the dispersion recovered by Grimme's D3 semiempirical approach.
[d] The values reported in this entry are the sum of the values of "DFT dispersion" and "Grimme dispersion".

Table S3. Energy decomposition analysis of the interaction energy between PDTA radicals in different configurations[a] of their isolated π-dimers. All components of the interaction energy are given in kcal mol^{-1}.

	Conf. A	Conf. B	Conf. C
Electrostatic	-11.32	-6.61	-5.38
Exchange	-9.33	-5.18	-4.03
Repulsion	50.21	29.10	22.84
Polarization	-15.12	-5.15	-4.65
DFT dispersion[b]	-14.46	-8.77	-7.44
Grimme dispersion[c]	-9.20	-8.02	-7.04
Total dispersion[d]	-23.66	-16.79	-14.48
Total interaction energy	-9,21	-4,64	-5,68

[a] The configurations are those marked by A, B and C in Figure S11 of the main text.
[b] This accounts for the dispersion that the PBE functional is able to recover by itself.
[c] This accounts for the dispersion recovered by Grimme's D3 semiempirical approach.
[d] The values reported in this entry are the sum of the values of "DFT dispersion" and "Grimme dispersion".